https://doi.org/10.1016/j.jhydrol.2019.124003

A general framework of design flood estimation for cascade reservoirs in operation period

Feng Xiong[1], Shenglian Guo[1]*, Pan Liu[1], C-Y Xu[2], Yixuan Zhong[1], Jiabo Yin[1], Shaokun He[1]

[1] State Key Laboratory of Water Resources and Hydropower Engineering Science；Wuhan University, 430072, China; [2]Dept. of Geosciences, University of Oslo, N-0316, Oslo, Norway. *Correspondence to slguo@whu.edu.cn

Abstract: The hydrological regimes of downstream reservoirs have been significantly altered due to the operation and regulation of upstream cascade reservoirs. The original design flood quantiles, namely “design flood in construction period”, do not consider anthropogenic impacts in reservoir operation period, and have led to enormous conflicts between flood control and conservation. In this study, the “design flood and flood limited water level in operation period” are defined for practical application. We establish a general framework to measure the spatiotemporal pattern of streamflow and to estimate design floods of cascade reservoirs in operation period. The multivariate t-copula and a genetic algorithm strategy are proposed to solve the curse of dimensionality encountered in the derivation of most likely regional composition. The Jinsha River and Yalong River cascade reservoir system in China, which consists of 13 large reservoirs with the total storage capacity of 74.06 billion m^3 and hydropower capacity of 71.47GW, is selected as a case study. Results indicate that: (1) The curse of dimensionality can be well addressed by applying multivariate t-copula to build high dimensional joint distribution and using the genetic algorithm to achieve the most likely regional composition. (2) Compared with the design floods in

construction period, the design floods of downstream reservoirs in operation period have been significantly reduced due to the upstream reservoir regulation. The 1000-year design peak flood discharge, 3-day, 7-day and 30-day flood volumes of Xiangjiaba reservoir decrease by 38.7%, 37.4%, 34.2% and 13.8%, respectively. (3) The flood limited water level of these reservoirs can be raised without increasing flood control risks in operation period. The cascade reservoirs in the Jinsha River and Yalong River can generate 3.28 billion kW·h more hydropower (or increase 4.3%) annually during flood season.

Key words: Cascade reservoirs; Design flood; Most likely regional composition; Flood limited water level; Multivariate t-copula; Genetic Algorithm

1 Introduction

Reservoirs are one of the most efficient infrastructure components for integrated water resources management (Guo et al., 2004; Liu et al., 2015). In recent decades, more and more reservoirs have been built for flood control and hydropower generation purposes and to meet the social economic development, forming a large quantity of cascade reservoir systems throughout the world (Zhao et al. 2016; Liu et al. 2016; Yazdi and Moridi, 2018). The function of reservoirs, in terms of flood water utilization, has become increasingly important (Li et al., 2010; Ouyang et al., 2015).

Reservoirs have significant impact on hydrological characteristics, especially the temporal variation of maximum stream flows (Gao et al., 2019). With the formation of

substantial numbers of cascade reservoir systems, the hydrological regimes of downstream section have been significantly altered. The statistical properties (e.g. mean, variance, skewness) of the extreme flood series of downstream reservoir in operation period are considerably different from the annual maximum data series adopted for “design flood in construction period” (Liang et al., 2018). Therefore, the investigation on “design flood in operation period” is of great significance in terms of scientific reservoir management.

The flood limited water level (FLWL) in construction period, which is determined by the reservoir regulation of the annual design flood hydrographs for given return period, serves as the most vital parameter of tradeoff between flood control and conservation (Yun and Singh, 2008; Li et al., 2010). During the flood season, the reservoir water level is not allowed to exceed the FLWL in order to offer adequate storage for possible incidences of large floods (Liu et al., 2015). The FLWL in construction period gives too much priority to low probability floods, which makes it a great challenge for reservoirs to produce the level of benefits that provides the economic justification for their development (Liu et al. 2015). With the formation of cascade reservoir systems, the application of FLWL in construction period has led to greater conflicts between flood control and water resources utilization. For example, the downstream reservoirs in a cascade reservoir system are often unable to refill to the normal water level by the end of refilling period under circumstances where all cascade reservoirs compete to impound water (Zhou et al., 2015), which largely limits

the comprehensive benefits of these reservoirs. Therefore, it is valuable to find the appropriate "FLWL in operation period" for raising water resources comprehensive utilization rate.

Recognizing the drawbacks of "design flood and FLWL in construction period", the "design flood and FLWL in operation period" are defined for practical application in this study. Yet only a handful of studies made preliminary attempts to study the reservoir impacts on downstream design floods which can be classified into three categories. The first option is based on the non-stationary flood frequency analysis framework with the "Reservoir Index" to represent the impacts of reservoir (López and Francés, 2013; Zhang et al., 2015; Wang et al., 2017). The Reservoir Index can be taken into account in a generalized addictive model as an effective covariate to study the reservoir impacts. Nevertheless, all the variables in a Reservoir Index series are constants in a specific period regardless of reservoir regulation strategies (Su and Chen, 2019). Therefore, the Reservoir Index may not be capable of accounting for the complex joint operation strategies of a cascade reservoir system. The second option is to derive flood frequency distributions resulting from reservoir impacts by applying linear and nonlinear reservoir models (Gao et al., 2019). However, the linear and nonlinear models are both the simplification of reservoir operation rules (Basha, 1994) and thus remain non-ignorable biases from actual situation (Kim and Georgakakos, 2014). These differences could be further significantly amplified due to the high-dimensional and nonlinear features of cascade reservoir system. The third option

is to study the reservoir impacts based on the flood regional composition (FRC) framework (Guo et al., 2018). The FRC framework aims at analyzing the flood generation mechanism of the investigated reservoir. The inflow of the investigated downstream reservoir comprises the inflow of upstream reservoir and all intermediate basin inflows between reservoirs. The upstream reservoir inflow can be transformed into outflow according to man-made reservoir operation rules. The design flood of the investigated downstream reservoir in operation period is influenced by: (1) the characteristics of upstream reservoirs (flood control storage, operation rules etc.); (2) the FRC of the reservoir. Therefore, the methods based on the FRC framework aim to seek an appropriate FRC from all possible compositions that satisfy water balance equation. Guo et al. (2018) derived theoretical formula to achieve the most likely regional composition (MLRC) method for triple cascade reservoirs and evaluated the reservoir operation impacts based on the MLRC results. The MLRC assumes that FRCs may differ in terms of their probabilities of occurrence, which can be measured by the value of joint probability density function of floods occurring at all sub-basins, and the FRC with the largest occurrence probability should be selected. Based on this assumption, Guo et al. (2018) adopted the asymmetric Archimedean copula to build the joint distribution of floods occurring at all sub-basins and used the Newton iteration method to seek for the optimal solution of the MLRC. Guo's method with strong statistical basis is likely to be implemented for practical use, but the barriers are twofold for derivation of MLRC as the number of cascade reservoirs increases: (1) the

asymmetric Archimedean copula adopted to build the joint distributions in Guo's study will bring large modelling errors triggered by the uncertainty of nesting structure and inability to be fully nested in high dimension (Serinaldi and Grimaldi, 2007; Hofert and Pham, 2013). (2) The Newton iteration method adopted in Guo's study is not capable of obtaining the optimal solution of the formula in high dimension due to the local convergence of the method (Dembo et al., 1982; Pilanci and Wainwright, 2017; Bottou et al., 2018).

Therefore, the curse of dimensionality has become the main problem to be addressed in the literature. It is essential to conduct in-depth research with state-of the-art techniques to conquer these challenges. In this study, we focus on overcoming the curse of dimensionality based on Guo's method due to its ease of implementation and potentiality in practical application. The abovementioned two bottlenecks caused by high dimensionality in deriving MLRC are addressed by selecting the multivariate t-copula to build the joint distribution and by applying a genetic algorithm (GA) based method. The multivariate t-copula belongs to the meta-elliptical class and can be easier extended to higher dimension compared with Archimedean copulas (Serinaldi et al. 2009). Moreover, the empirical fit of the t-copula is often good and is almost always superior to that of the Gaussian copula (Mashal et al. 2003, Breymann et al. 2003). The t-copula has been given more attention recently due to its favorable empirical fit and ease of implementation (e.g. Zhang et al., 2016; Rivieccio and Luca at al., 2016; Hao et al., 2017; He et al., 2017), and therefore is considered in this study.

The derivation of MLRC in higher dimension typically involves highly nonlinear and nonconvex problems. As opposed to the current formula-based technique adopted by Guo et al. (2018), we develop a GA-based method to obtain the robust solution of MLRC in higher dimension. The GA proposed by Holland (1975) has the ability to mimic processes observed in natural evolution and is prevalently utilized to address various optimization problems in hydrological practice (e.g. Yin et al., 2017; Ehteram et al., 2018; Zhou et al., 2019). Based on the derivation of MLRC in high dimension, we propose a general framework for deriving design floods for cascade reservoir system and determining the FLWL in operation period. To ensure that the results of MLRC are reasonable and can be adopted for practical use, the standard FRC method recommended by MWR (2006), i.e. equivalent frequency regional composition (EFRC) method is also applied and compared in this study.

This study is therefore explored with three foci: (1) introducing the "design flood and FLWL in operation period" to practical application in hydrology and (2) addressing the curse of dimensionality encountered in the derivation of MLRC by applying the multivariate t-copula and a GA-based strategy (3) developing a general framework for determining the design flood of cascade reservoirs in operation period. The present paper is structured as follows. Section 2 describes the methodology used in this study. Section 3 briefly introduces the study area and the material. In Sections 4, a mix cascade reservoir system in the Jinsha River and Yalong River in China is selected as a case study. The impact of upstream reservoir regulation on design floods

as well as the FLWLs of downstream reservoirs are analyzed and discussed. The last two sections are devoted to the discussion and conclusion of this study, respectively.

2. Methodology

2.1 Design flood in operation period

The similarities and differences between design flood in construction period and in operation period are compared in Table 1. The purpose of design flood in construction period is to provide vital information for the design of the reservoir storage, spillway size etc. While the design flood in operation period considers the impact of upstream reservoir operation and thus is capable of adapting to the variation of upstream hydrological regime, and its main purpose is to counterbalance the conflicts between flood control and conservation. In terms of property, the design flood in construction period and in operation period are both static values which are unchanged over time, and therefore can be easily implemented for practical use. By applying FLWL in construction period, the reservoir can regulate low frequency design floods, but the comprehensive benefits of reservoir storage cannot be fully utilized. By applying FLWL in operation period, the reservoir can withstand the same frequency floods regulated by upstream reservoirs and gain more comprehensive benefits during the flood season. To summarize, the main difference between the design flood in construction period and in operation period is that the latter considers the impact of upstream reservoir regulation and tends to be more rational than the

169 former in terms of flood water utilization.

170 **2.2 Derivation of design flood in operation period**

171 **2.2.1 Framework**

172 The main goal of this study aims at exploring a general framework for estimating
173 design flood for a cascade reservoir system in operation period, in which the curse of
174 dimensionality is the main task to be addressed. The architecture of the proposed
175 framework is shown in Fig. 1, which comprises three modules, namely: (1) design
176 flood in construction period module; (2) flood regional composition (FRC) module,
177 and (3) design flood in operation period module. The first module is responsible for
178 calculating the design flood peak, volumes and design flood hydrographs in
179 construction period for the second and third modules, respectively. In this study, the
180 design floods both in operation and construction periods are analyzed for the given
181 same return periods and flood prevention standards. The second module is responsible
182 for obtaining the FRC of the investigated reservoir. In this module, the multivariate
183 t-copula is proposed to build high dimensional joint distributions and a GA-based
184 method is proposed to derive the MLRC. The EFRC method suggested by MWR
185 (2006) is also applied in this module for comparative study. Finally, the design flood
186 and FLWL in operation period is calculated in the last module based on the design
187 flood hydrographs in construction period obtained in the first module and the FRC
188 results obtained in the second module. By regulating the design flood hydrographs in

construction period with the consideration of the operation rules of upstream cascade reservoirs, the complex impact of reservoir regulation on downstream reservoir design flood can be numerically evaluated in this module. The main procedures and detailed explanations are given as follows.

2.2.2 Design flood in construction period module

The general methodology of estimating design flood in construction period is to fit the flow data, such as the annual maximum (AM) data using a theoretical probabilistic distribution and derive the exceedance probability based on the selected distribution (Xiong et al., 2018). The Pearson type 3 (P3) distribution and curve fitting estimation method is recommended by Ministry of Water Resources (MWR, 2006) as the standard hydrological frequency analysis procedure in China and thus is adopted in this study. Compared with commonly used methods, such as L-moments and maximum likelihood method, the curve fitting method can easily incorporate historical and paleo flood information while guarantee satisfactory statistical properties of the estimation results (Hu, 1987, Hua 1987). The Kolmogorov–Smirnov (KS) test and Anderson-Darling (AD) test are selected as the goodness-of-fit statistics to determine whether the candidate variables follow the P3 distribution (Zhang and Singh, 2007; Huang *et al*., 2018b). From the perspective of engineering safety, the flood which may lead to serious damage would be preferred when selecting typical flood hydrograph for reservoir design purpose (MWR, 2006, Xiong et al., 2019). Severe floods occurred in both the mainstream and main tributaries of Jinsha River in

1966 flood season. Therefore, the 1966 flood hydrograph is selected as the typical flood hydrograph in this study.

2.2.3 Flood regional composition module

2.2.3.1 Flood regional composition for cascade reservoirs

The flood regional composition (FRC) has been recommended by MWR (2006) to solve a wide range of problems for the following reasons: (1) Methods based on the FRC are easy to implement (Lu et al., 2012). (2) Methods based on FRC can provide numerical solutions even for highly complex problems such as calculating the flood control effects of reservoir on downstream section and analyzing the joint operation strategies of cascade reservoirs or reservoir group, which is essential for the engineering practice (Guo et al., 2018).

The sketch diagram of cascade reservoirs is given in Fig. 2. In general, a more complex hybrid reservoir group can be decomposed into several cascade reservoirs based on large scale system theories (Chen *et al.*, 2017). Let A (A_1, A_2, …, A_n), B (B_1, B_2, …, B_n) and C denote the reservoirs, intermediate basins and downstream reservoir site of interest, respectively, and let random variables X_1, X_2, …, X_n, Y_1, Y_2, …, Y_n and Z represent the natural flood volumes of reservoirs A_1, A_2, …, A_n, intermediate basins B_1, B_2, …, B_n and downstream reservoir C with the corresponding values x_1, x_2, …, x_n, y_1, y_2, …, y_n and z, respectively.

We focus on the A1-A2 sub-system to further demonstrate the FRC concept. The

design flood of downstream reservoir A2 is impacted by the regulation of upstream reservoir A1. The inflow of downstream reservoir A2 is composed of inflow of upstream reservoir A1 and intermediate basin inflow B1. Thus (x_1, y_1) is the FRC of x_2, in which x_1 can be transformed into outflow based on the operation rules of A1. Therefore, the statistical behavior of design flood of downstream reservoir A2 in operation period is deterministically related to the FRC of A2, i.e. (x_1, y_1).

For the cascade reservoir system, according to the principle of water balance equation, all the FRC (x_1, y_1, y_2, … y_n, z) should be subjected to the following equations:

$$\begin{aligned} & x_1 + y_1 = x_2 \\ & x_1 + y_1 + y_2 = x_3 \\ & \ldots \\ & x_1 + y_1 + y_2 + \ldots + y_n = z \end{aligned} \tag{1}$$

Due to the inherent stochastic nature of flood generation mechanism, there are countless compositions of (x_1, y_1, y_2, … y_n, z) aligning with the principle of water balance. In order to search for a representative FRC which is consistent with the spatiotemporal pattern of streamflow, two FRC methods based on different assumptions are considered in this study and are introduced hereafter.

2.2.3.2 Equivalent Frequency Regional Composition (EFRC) method

The EFRC method assumes that the return period of flood occurring at one of the subareas (reservoir or the intermediate basin) is the same as the downstream reservoir. Though easy to implement, the EFRC suffers from two main drawbacks (Guo et al.,

2018): (1) It assumes perfect correlation between floods occur at one sub-basin and downstream site, which does not always conform to the reality; (2) For the composition of cascade reservoirs, the number of EFRCs (2^n-1) increases exponentially with the increase of the number of cascade reservoirs (n). In this study, only one representative EFRC for cascade reservoirs, namely EFRC-1 is considered for the purpose of comparison. For a given return period, the floods occurring at all reservoirs x_1, x_2, …, x_n, z can be determined by their respective fitted distributions. The floods occurring at all intermediate basins y_1, y_2, …, y_n can be calculated using the water balance equation. EFRC (x_1, y_1, y_2, …, y_n) can thus be determined. Readers can refer to Liang *et al*. (2017) and Guo *et al*. (2018) for more details about the EFRC method.

2.2.3.3 Most Likely Regional Composition (MLRC) method

To overcome the drawbacks of EFRC, Guo et al. (2018) proposed the MLRC based on copulas. They indicated that: (1) The MLRC method with stronger statistical basis can better capture the actual spatial correlation of flood events occurring at different sub-basins; (2) The composition of MLRC method is unique, and thus is easy to implement for large cascade reservoir system. The MLRC method assumes that FRCs may differ in terms of their probability of occurrence, which can be measured by the value of joint probability density function of random variables X_1, X_2, …X_n, Z, i.e. $f(x_1, x_2, …, x_n, z)$. According to Sklar's theorem (Nelsen, 2006), the joint probability density function can be expressed in terms of its marginal

distributions and the associated dependence function, i.e. copula function as follows (Salvadori *et al.*, 2004, 2016)

$$f(x_1, x_2, \cdots, x_{n-1}, x_n, z) = c(u_1, u_2, ..., u_{n-1}, u_n, v) \prod_{i=1}^{n} f_{X_i}(x_i) \cdot f_Z(z) \quad (2)$$

where c is the PDF of copula function and u_1, u_2, …, u_n, v are the corresponding empirical frequencies of x_1, x_2, …, x_n, z. $f_{X_i}(x_i)$ (i=1, 2, …, n) and $f_Z(z)$ are the marginal distributions of floods occurring at reservoirs A_1, A_2… A_n and downstream reservoir C, respectively.

The composition (x_1, x_2, …, x_n, z) is more likely to occur when the value of density function f(x_1, x_2, …, x_n, z) increases (Salvadori *et al.*, 2011). In order to search for the MLRC, the f(x_1, x_2, …, x_n, z) is maximized by subjecting water balance constraint in Equation (1) for the given $Z = z_p$

$$\left.\begin{array}{ll} max & f(x_1, x_2, \cdots, x_{n-1}, x_n, z) = c(u_1, u_2, ..., u_{n-1}, u_n, v) \prod_{i=1}^{n} f_{X_i}(x_i) \cdot f_Z(z) \\ s.t. & x_1 + y_1 = x_2 \\ & x_1 + y_1 + y_2 = x_3 \\ & ... \\ & x_1 + y_1 + y_2 + ... + y_n = z = z_p \end{array}\right\} \quad (3)$$

where z_p is the design flood volume for a given return period of the investigated reservoir obtained from the design flood in construction period module.

The joint probability density f(x_1, x_2,…, x_n, z) is maximized when its first order derivative equals zero and the following equation should be satisfied

$$\left.\begin{array}{l} \frac{\partial f(x_1, x_2, \cdots, x_{n-1}, x_n, z)}{\partial x_1} = 0 \\ \frac{\partial f(x_1, x_2, \cdots, x_{n-1}, x_n, z)}{\partial x_2} = 0 \\ \cdots \\ \frac{\partial f(x_1, x_2, \cdots, x_{n-1}, x_n, z)}{\partial z} = 0 \\ s.t. \quad \begin{array}{l} x_1 + y_1 = x_2 \\ x_1 + y_1 + y_2 = x_3 \\ \cdots \\ x_1 + y_1 + y_2 + \ldots + y_n = z = z_p \end{array} \end{array}\right\} \quad (4)$$

After the composition (x_1, x_2, …, x_n, z) is derived from Equation (4), MLRC (x_1, y_1, y_2, …, y_n) can be determined using the water balance equation.

As indicated previously, Guo's method suffers from curse of dimensionality as the number of cascade reservoirs increase. In this study, the curse of dimensionality is addressed by the following flow chart as shown in Fig 3, and the main procedures are described as follows:

(1) Determine the marginal distributions and joint distribution according to the sampled AM data series;

The vine-copula and meta-elliptical copula are often used to establish a higher dimensional joint distribution. The vine copula embraces a large quantity of pair-copula decompositions for high-dimensional variables, which makes the selection of suitable vine composition considerably complex (Aas *et al*., 2009). On the other hand, the meta-elliptical copula can model arbitrary pairwise dependence structures through a correlation matrix and is easy to implement (Huang *et al.*, 2018a). Considering the advantage of meta-elliptical copula and the drawback of vine copula, the meta-elliptical copula is selected in this paper. Gaussian copula and t-copula are

the commonly used meta-elliptical copulas. Mashal *et al.* (2003) and Breymann *et al.* (2003) have shown that the goodness-of-fit of the t-copula is almost always superior to that of the Gaussian copula. Serinaldi *et al.* (2009) and Chen *et al.* (2016) also indicated that t-copula is adequate to construct high dimensional joint distribution. Hence, the t-copula is employed to establish the joint distribution of the flood volumes of different sub-basins in this study.

The maximum likelihood method is adopted to estimate parameters of t-copula (Huang et al., 2018a). The goodness-of-fit of t-copula is assessed with the KS test and Cramer-von Mises (CM) test (Genest et al., 2008, 2009). The degree of freedom of t-copula is selected under the criteria of the Root Mean Square Error (RMSE) and Akaike Information Criterion (AIC) (Xiong *et al.*, 2018b; Zhong *et al.*, 2018). The smaller RMSE and AIC represents the better performance of the candidate model.

(2) In order to find the optimal composition of flood volumes [x_1^*, x_2^*, …, x_n^*] that maximizes the joint probability density function, the negative value of joint probability density is set as the fitness function, and the flood volumes of the upstream reservoirs [x_1, x_2, …, x_n] is set as the parameters to be optimized. Considering the water balance equations should always be satisfied in FRC, the water balance equations are employed as constraints to determine the initial value and threshold of the parameters. The fitness function and constraints are expressed as follows

$$\left.\begin{aligned} \min \quad & -f(x_1, x_2, \cdots, x_{n-1}, x_n, z) = -c(u_1, u_2, ..., u_{n-1}, u_n, v)\prod_{i=1}^{n} f_{X_i}(x_i) \cdot f_Z(z) \\ s.t. \quad & x_1 + y_1 = x_2 \\ & x_1 + y_1 + y_2 = x_3 \\ & ... \\ & x_1 + y_1 + y_2 + ... + y_n = z = z_p \end{aligned}\right\} \quad (5)$$

where the corresponding empirical frequencies [u_1, u_2, …, u_n] can be expressed with respect to their marginal distributions.

The formula-based derivation of MLRC for an *n*-dimensional cascade reservoir system adopted by Guo et al. (2018) is substantially equivalent to solving a set of *n*-dimensional nonlinear and nonconvex equations, and the optimal solution can be hard to achieve by the Newton iteration method due to its inherent drawbacks of local convergence and susceptibility to initial solution. The GA-based method in this study, however, can effectively achieve the computational complexity reduction by transforming the derivation process into an optimization process. The GA technique has proved to be capable of coping with highly complex optimization problems (Chang et al., 2003, 2005; Ghareb et al., 2016). Attaining the MLRC of *n*-dimensional cascade reservoir system corresponds to an optimization problem with *n* parameters to be optimized, and currently the number of reservoirs *n* is usually less than 20. Moreover, different initial conditions have been considered to test whether the optimal solution is robust. Results indicate that when using different initial seeds, the obtained optimal solutions show no significant difference. Therefore, the GA-based method can be effectively applied to existing cascade reservoir systems.

2.2.3.4 Comparison of EFRC and MLRC

The basic cascade reservoir system (see sub-system A1-A2) with synthetic inflow time series are used to compare the EFRC and MLRC methods. Since both EFRC and MLRC methods focus on the analysis of AM data series, we adopt the following procedures to generate AM flood series of A1 and A2 with different correlations for comparison. Firstly, the margins of A1 and A2 are assumed to be P3 distribution and the location, scale, shape parameters of P3 distribution for A1 (A2) reservoir are assumed to be 30 (50), 7.5 (12.5) and 4 (4), respectively. Secondly, two sets of uniform variables over (0, 1) are randomly generated from a bivariate t-copula with sample size M=60 using R package "Copula" (Demarta and McNeil, 2005; Yan, 2007), which are considered as the empirical frequencies of the AM flood series of the two reservoirs. And the correlation coefficients between the two sets of uniform variables are set to be 0.01, 0.3, 0.6 and 0.99 respectively to demonstrate AM flood series with different correlations. Finally, the AM flood series of the two reservoirs can be generated by applying the predetermined P3 quantile functions to the obtained uniform variables with the consideration of noise term. The EFRC and MLRC methods are used to analyze the FRC of 1000-year design flood of A2 inflow and results are summarized in Table 2. It can be seen from Table 2 that when the correlation coefficient between the AM floods of A1 and A2 is extremely high (0.99), the results obtained by MLRC and EFRC are nearly the same. However, when the correlation is very weak (0.01), the differences between results of MLRC and EFRC

are significant, i.e. the "equivalent frequency assumption" adopted by EFRC is unreasonable for weak correlated floods (MWR 2006). Thus, the MLRC method enabling to consider the actual correlation between AM floods may offer more reasonable results compared with EFRC.

2.2.4 Design flood in operation period module

The main procedures of this module are described as follows:

(1) Derive the corresponding design flood hydrographs of each sub-basin using the peak and volume amplitude (PVA) method (Zhong *et al*., 2017; Yin *et al*., 2018) based on the FRC results and design flood hydrographs in construction period. The advantage of PVA method is that it ensures that both the flood peak and volume are equal to the assigned values without modifying flood duration (Yin *et al*., 2018).

(2) Obtain the design flood hydrograph at the downstream site C based on river channel flood routing and reservoir flood regulation. The commonly used Muskingum model is considered for the river channel flood routing (Franchini *et al*., 2011; Guo *et al*., 2018). Then the design peak flood discharge and volumes are directly determined from the design flood hydrograph in operation period to offer a numerical estimation of design flood.

(3) Determine the FLWL in operation period using the iterative calculation method (Xiao *et al*., 2009; Zhou *et al*., 2015) according to the derived design flood hydrograph and the reservoir operation rules. The flood prevention standard cannot be lowered down under the iterative calculation approach (Zhou *et al*., 2015).

3. Study area and materials

Jinsha River is the upper reach of Yangtze River and has a total length of 3481 km with a drainage area of 502,000 km^2, accounting for 26% of the drainage area of the Yangtze River. The Jinsha River is divided into upper, middle and lower reaches with respective lengths of 965 km, 1220 km and 1296 km. Yalong River is the largest tributary of Jinsha River with a drainage area of 136,000 km^2. During the past decades, a series of dams have been built along the main Jinsha River and Yalong River for the purpose of flood control and hydropower generation. Among them the Liyuan (LY), Ahai (AH), Jinanqiao (JAQ), Longkaikou (LKK), Ludila (LDL) and Guanyinyan (GYY) reservoirs are located in the midstream Jinsha River; while the Wudongde (WDD), Baihetan (BHT), Xiluodu (XLD) and Xiangjiaba (XJB) reservoirs are located in the downstream Jinsha River. Along the Yalong River, there are Lianghekou (LHK)-Jinping (JP)-Ertan (ET) cascade reservoirs. The investigated area and sketch map of cascade reservoirs in the Jinsha River and Yalong River are shown in Fig. 4. The basic information of these reservoirs is listed in Table 3. To promote water resources utilization and hydropower generation, these 13 mega cascade reservoirs have been jointly operated to achieve a total reservoir storage of 74.06 billion m^3 (21.82 billion m^3 for flood control) and a total installed hydropower capacity of 71.47 GW. The current operation rules (standard operation policy) of these reservoirs are provided by the Changjiang (Yangtze River) Water Resources Commission (CWRC), Ministry of Water Resource (CWRC, 2018). The data sets used in this study are

natural daily streamflow data of the investigated dam sites with record lengths all longer than 50 years. The data sets are provided by the CWRC and have been widely used for the design and management of these reservoirs.

4. Result analysis

4.1 The design flood in construction period

According to the regulation characteristics of cascade reservoirs in the Jinsha River and Yalong River, annual maximum 7-day and 30-day (denoted as AM 7d and AM 30d) flood volume series are selected for flood frequency analysis. The *P*-values of KS and AD tests of each variable are calculated. For both of the tests, when *P*-value is larger than 0.05, the assumption that the AM series follows the P3 distribution cannot be rejected at a 5% significance level. For illustration only, the cumulative distributions of AM 7d flood volumes series fitted by P3 distributions for AH, LKK, GYY, ET. BHT and XJB reservoirs are plotted in Fig. 5. The figure shows a good correspondence between empirical and theoretical frequencies and the assumption that the variables follow the P3 distribution cannot be rejected.

4.2 Design flood of cascade reservoirs in the midstream Jinsha River and Yalong River

4.2.1 Flood regional composition

There are no intermediate inflows from tributaries between cascade reservoirs in the midstream Jinsha River and Yalong River (Fig. 4) and the FRC for these reservoirs

424 can be directly analyzed by the general form (Fig. 2). The FRC of AM 7d and 30d
425 flood volumes of each reservoir in the midstream Jinsha River and Yalong River are
426 analyzed. Taking the FRC of GYY reservoir as an example, the flood volume of GYY
427 reservoir (X_6) is decomposed to: LY reservoir (X_1), L-A inter-basin (Y_1), A-J
428 inter-basin (Y_2), J-L inter-basin (Y_3), L-L inter-basin (Y_4), and L-G inter-basin (Y_5).

429 Taking the establishment of joint distribution for the MLRC of GYY reservoir as
430 an illustration, the *P*-values of KS and CM tests, RMSE and AIC values of t-copulas
431 with different degrees of freedom are calculated and listed in Table 4. It can be seen
432 that all *P*-values are greater than 0.05, indicating that the variables following t-copula
433 cannot be rejected at a 5% significance level. Table 4 indicates that the t-copula with
434 v=3 degrees of freedom exhibits the smallest RMSE and AIC, and thus should be
435 selected. The adequacy of the t-copula is further evaluated with the P-P plots by
436 plotting the empirical copula against theoretical copula (Van *et al.*, 2018). For
437 illustration only, Fig. 6 shows the P-P plots of joint distributions for the MLRC
438 method of AH, LKK, GYY and ET reservoirs, respectively. The *P*-values obtained
439 from KS and CM tests are also shown. It can be seen from Fig. 6 that all *P* values of
440 all t-copulas are greater than 0.05, and no strong departure from the expected
441 distribution can be observed from the P-P plots. Therefore, the t-copula can be
442 effectively implemented for establishing joint distributions in high dimension.

443 Following the procedures described in Section 2.2.3, the EFRC and MLRC
444 methods of AM 7d and 30d flood volumes of cascade reservoirs are obtained. Taking

the FRC of AM 7d flood volumes of GYY reservoir as an example, it can be observed from Table 5 that the results obtained by the EFRC and MLRC methods show no significant difference in this case study. The similarity between the results of EFRC and MLRC is due to the fact that there exist strongly positive correlations between the flood volumes of downstream reservoir and its upstream reservoirs, and this will be further discussed in Section 5.1.

Regarding the curse of dimensionality, Guo's method is compared with the proposed method for deriving MLRC with different numbers of cascade reservoirs, taking the derivation of MLRC of AH (2 reservoirs) and LDL reservoirs (5 reservoirs) as illustrations. The MLRC derived by Guo's method and the proposed method are compared in Table 6. As for the derivation of MLRC for AH reservoir, the results obtained by the two methods are nearly the same. This indicates that the solutions of the proposed method are reliable. As for the derivation of MLRC for LDL reservoir, Guo's method cannot obtain the solution of MLRC, while the proposed method can effectively achieve the MLRC of LDL reservoir. This demonstrates that Guo's method can be subject to the curse of dimensionality as the number of cascade reservoirs increases, which can be well addressed by the proposed method.

4.2.2 Reservoir design flood in operation period

The impact of upstream reservoir operation can be analyzed following the procedures described in Section 2.2.4. The original design flood frequencies of cascade reservoirs in the midstream Jinsha River and Yalong River are 0.2% (return

period is 500-year) and 0.1% (return period is 1000-year), respectively. The design frequency floods in construction period and in operation period are compared in Table 7. Results indicate that:

(1) The estimated design peak flood discharge (Q_{max}), 3-day (W_3), 7-day (W_7) and 30-day (W_{30}) flood volumes of downstream reservoirs decrease due to the upstream reservoir operation. For instance, the estimated Q_{max}, W_3, W_7 and W_{30} of GYY reservoir in operation period decrease by 11.5%, 9.7%, 7.3% and 0.4%, respectively compared with the design values in construction period.

(2) The reduction rates of downstream reservoirs are greater than that of the upstream reservoirs. This is as expected that when the available flood control storage is larger, the flood can be better regulated.

(3) The FLWL of downstream reservoirs in operation period is higher than that of the designed values in construction period. The FLWLs of AH, JAQ, LKK, LDL, GYY, JP and ET reservoirs in operation period (in construction period) are 1493.7 (1493.3) m, 1410.8 (1410) m, 1290.3 (1289) m, 1212.8 (1212) m, 1123.5 (1122.3) m, 1862.4 (1859) m and 1191.6 (1190) m respectively. The less required flood control storage accounts for the raise of FLWLs in operation period.

(4) Under the FLWL scheme in operation period, the AH, JAQ, LKK, LDL, GYY, JP and ET reservoirs increase the hydropower generation by 0.45%, 0.72%, 2%, 1.1%, 1.2%, 1.6% and 0.6%, respectively. It can be summarized from Table 7 that the cascade reservoirs in the midstream Jinsha River and Yalong River can increase

annual hydropower generation (HG) by 126 million kW·h in flood season in operation period.

4.3 Design flood of cascade reservoirs in the downstream Jinsha River

4.3.1 Flood regional composition

The inflows of cascade reservoirs in the downstream Jinsha River are impacted by both the cascade reservoirs in the midstream Jinsha River and Yalong River (see Fig. 4), and it would not be possible to carry out FRC analysis without decomposition (Chen et al., 2017). The FRC of WDD, BHT, XLD and XJB reservoirs follows a three-step procedure described as below, taking the FRC of XJB reservoir as an illustration:

Firstly, the flood volume of XJB (X_{13}) is decomposed to: WDD reservoir (X_{10}), W-B inter-basin (Y_9), B-X inter-basin (Y_{10}) and X-X inter-basin (Y_{11}). Secondly, the flood volume of WDD reservoir (X_{10}) is decomposed to: GYY reservoir (X_6), ET reservoir (X_9) and G-E-W inter-basin (Y_8). Finally, the flood volume of GYY reservoir (X_6) is decomposed to: LY reservoir (X_1), L-A inter-basin (Y_1), A-J inter-basin (Y_2), J-L inter-basin (Y_3), L-L inter-basin (Y_4), and L-G inter-basin (Y_5); and the flood volume of ET reservoir (X_9) is decomposed to: LHK reservoir (X_7), L-J inter-basin (Y_6) and J-E inter-basin (Y_7). The FRC of GYY and ET reservoirs has been achieved in Section 4.2.

The EFRC and MLRC are adopted to obtain the FRC of these reservoirs following the decomposition procedure. Fig. 7 shows the goodness-of-fit of the

selected t-copula. Table 8 lists the results of FRC, using the XJB reservoir as an example. Results from Fig. 7 and Table 8 reveal again that: (1) The t-copula can be effectively implemented to establish the joint distributions for MLRC of the investigated reservoir. (2) The MLRC method can be effectively implemented for the complex hybrid reservoir system.

4.3.2 Design flood in operation period

The design flood return periods of cascade reservoirs in the downstream Jinsha River are all 1000-year. The 1000-year design flood hydrographs of WDD, BHT, XLD and XJB reservoirs in construction period and in operation period are compared in Fig. 8. The statistics of the 1000-year design floods in construction period and the estimated design floods in operation period are summarized in Table 9. Results show that:

(1) The 1000-year design flood hydrographs of the four reservoirs alter considerably in operation period with smaller flood peaks and gentler flood processes.

(2) The 1000-year design Q_{max}, W_3, W_7 and W_{30} of the four reservoirs decrease significantly due to the upstream reservoir operation. For instance, the 1000-year design Q_{max}, W_3, W_7 and W_{30} of XJB reservoir decrease by 38.7%, 37.4%, 34.2%, 13.8%, respectively in operation period. Compared with the cascade reservoirs in the midstream Jinsha River and Yalong River, greater significant reduction rates are observed.

(3) Due to the significant decrease in design floods, the FLWL of the four

reservoirs in operation period can be largely raised. The FLWLs of WDD, BHT, XLD and XJB reservoirs in operation period (in construction period) are 958.01(952) m, 793.6(785) m, 572.71(560) m and 372.09(370) m, respectively.

(4) Under the FLWL scheme in operation period, the WDD, BHT, XLD and XJB reservoirs can increase the hydropower generation (HG) by 4.7%, 4.8%, 7.2%, and 2.2%, respectively. It can be summarized from Table 9 that the cascade reservoirs in the downstream Jinsha River can increase annual hydropower generation by 3.15 billion kW·h during flood season in reservoir operation period.

5 Discussion

5.1 Analysis of EFRC and MLRC results

As can be seen from Table 5, the results of EFRC and MLRC of GYY reservoir are analogous in this case study. This is because the inflow discharges are highly correlated as demonstrated in Section 2.2.3.4. The Kendall's tau correlation coefficients between the AM 7d flood volume series of cascade reservoirs in the midstream Jinsha River are calculated and listed in Table 10. It is indicated from Table 10 that the correlations are considerably strong, with the Kendall's tau correlation coefficients all greater than 0.7. The main reasons for the strong correlation are summarized as follows: (1) The drainage areas of these reservoirs are quite similar (Table 3) and there are no big tributaries between these reservoirs (Fig. 4). (2) They belong to the same rainfall zone and yield analogous climatic factors. Consequently,

549 the equivalent frequency floods at each reservoir site are likely to occur in this case
550 study and the EFRC method can be adopted for such catchment with high-correlated
551 inflows across all sub-basins. While the MLRC method which can be applied to both
552 high and low correlated sub-basin inflows is more rational than the EFRC method.

553 On the other hand, as noted before, different FRCs may differ in terms of their
554 occurrence probabilities, which can be measured by the value of joint probability
555 density function of floods occurring at all sub-basins (Guo et al., 2018). The larger
556 joint probability density function denotes the greater occurrence probability of the
557 FRC. In practical application, the FRC which is more likely to occur usually gains
558 more attention. Therefore, the occurrence probabilities of EFRC and MLRC for
559 design flood with different return periods are compared in Fig. 9. Taking the LKK and
560 GYY reservoirs as an example, it can be seen that the occurrence probabilities of
561 EFRC (MLRC) for design flood of LKK reservoir with return periods of 1000, 500
562 and 100-year are 2.32 (5.64) $\times 10^{-7}$, 3.48 (12.6) $\times 10^{-7}$ and 9.42 (22.04) $\times 10^{-7}$,
563 respectively; and the occurrence probabilities of EFRC (MLRC) for design flood of
564 GYY reservoir with return periods of 1000, 500 and 100-year are 1.35 (4.17) $\times 10^{-8}$,
565 2.76 (15.75) $\times 10^{-8}$ and 14.15 (56.6) $\times 10^{-8}$, respectively. When the floods with return
566 periods of 1000, 500 and 100-year occur at the LKK (GYY) reservoir, the occurrence
567 probabilities of MLRC are 2.43 (3.09), 3.62 (5.49) and 2.34 (4.0) times as large as
568 that of EFRC, respectively. This explicitly implies that the MLRC offers a meaningful
569 flood regional composition scheme with high occurrence probability. In terms of

570 occurrence probability, the MLRC performs much better than EFRC method.

571 **5.2 Relation between the reduction rates and available flood control storage**

572 The relation between the reduction rates of Q_{max}, W_3, W_7 and W_{30} and available
573 flood control storage are investigated and plotted in Fig. 10 in recognition that the
574 available flood control storage can largely influence the reduction rates. It can be
575 observed from Fig. 10 that:

576 (1) The Q_{max} and W_{30} are the most and least impacted by the available flood
577 control storage, respectively. This is mainly because a reservoir will store water to
578 reduce flood peak when a flood occurs, however not for a long period such as 30 days
579 in flood season.

580 (2) The reduction rates of designed Q_{max}, W_3, W_7 and W_{30} increase with the
581 increase of available flood control storage, while the increasing rate shows a
582 decreasing trend. The available flood control storages of the cascade reservoirs in the
583 downstream Jinsha River are considerably larger than that in the midstream Jinsha
584 River and Yalong River, and thus the reduction rates are also larger. The decreasing
585 trend in increasing rate is mainly because when the flood control storage is sufficient
586 for the flood control purpose, the flood can be well regulated and the reduction rate
587 will no longer increase with the increase of flood control storage.

588 **5.3 Practical application of FLWL in operation period**

589 In this study, it is shown that the formation of cascade reservoir system has

resulted in considerable attenuation effects on design floods of downstream reservoirs. With advancements in meteorological and hydrological forecasting capabilities, the operational efficiency of existing reservoir has been improved significantly, which creates the possibility for the practical application of FLWL in operation period. For example, on basis of real-time flood forecasting, a pre-release strategy can be adopted to bring substantial economic benefits without increasing flood control risks (Li et al., 2010; Chou and Wu, 2013). Based on the application experience, a pre-release strategy combined with hydrological forecasts can be adopted for practical application of FLWL in operation period. When recent hydrological forecasts indicate that no extreme flood (e.g. return period greater than 100-year) will occur, the reservoir can be operated within the FLWL in operation period; when extreme floods are forecasted to occur within the forecast horizon, reservoir can pre-release flood water to operate within the FLWL in construction period to ensure the safety of dam as well as downstream sections. This pre-release strategy has been widely used to better compromise between flood control and conservation, and it will be quantitatively investigated for practical application of FLWL in operation period in future work.

6 Conclusions

In this study, the “design flood and FLWL in operation period” are defined for practical application. A general framework enabling to measure the spatiotemporal pattern of streamflow for deriving the design floods in operation period for cascade

610 reservoirs is established. The multivariate t-copula and GA-based strategy are applied
611 to solve the curse of dimensionality involved in the derivation of MLRC. The hybrid
612 reservoir system in Jinsha and Yalong River is selected as the case study. The main
613 conclusions are summarized as follows:

614 (1) The multivariate t-copula can be effectively implemented for establishing
615 high dimensional joint distributions and the GA-based method can be adopted to
616 achieve the MLRC in high dimension. The proposed framework can be effectively
617 implemented for a complex cascade reservoir system.

618 (2) Compared with the design floods in construction period, design floods of the
619 downstream reservoirs in operation period have been reduced significantly due to the
620 regulation of upstream reservoirs. When the available flood control storage is larger,
621 the reduction rates of design floods are even greater. For instance, the 1000-year
622 design Q_{max}, W_3, W_7 and W_{30} of XJB reservoir decrease by 38.7%, 37.4%, 34.2%,
623 13.8%, respectively in operation period. Hence, the impact of upstream reservoir
624 regulation on downstream reservoir cannot be ignored, and the investigated reservoir
625 operation policy formulated based on the design flood in operation period should be
626 adopted.

627 (3) The FLWL in operation period can be raised compared with the design value
628 in construction period. The FLWLs of AH, JAQ, LKK, LDL, GYY, JP, ET, WDD,
629 BHT, XLD and XJB reservoirs in operation period (in construction period) are
630 1493.7(1493.3) m, 1410.8(1410) m, 1290.3(1289) m, 1212.8(1212) m, 1123.5(1122.3)

m, 1862.4(1859) m, 1191.6(1190) m 958.01(952) m, 793.6(785) m, 572.71(560) m and 372.09(370) m, respectively. The economic benefits obtained from the new FLWL scheme are enormous. As can be summarized from Table 5 and Table 7, the 13 reservoirs in the Jinsha River and Yalong River can increase the annual hydropower generation by 3.28 billion kW·h (or increase 4.3%) during flood season without increasing flood control risks.

Acknowledgments

This study was financially supported by the National Natural Science Foundation of China (51879192), the National Key Research and Development Plan of China (2018YFC1508001), the "111 Project" Fund of China (B18037) and the Research Council of Norway (FRINATEK Project 274310). The authors would like to thank the editors and anonymous reviewers for their constructive comments, which have led to significant improvement on the presentation and quality of the paper.

Reference

Aas, K., Czado, C., Frigessi, A., Bakken, H., 2009. Pair-copula constructions of multiple dependence. Insur. Math. Econ. 44, 182-198.

Basha, H.A. 1994. Nonlinear reservoir routing: particular analytical solution. J. Hydraul. Eng., 120(5), 624-632.

Bottou, L., Curtis, F., Nocedal, J. 2018. Optimization methods for large-scale machine learning. Siam Rev., 60(2), 223-311

Breymann, W., Dias, A., Embrechts, P. 2003. Dependence structures for multivariate high-frequency data in finance. Quant. Financ., 3, 1-14

Chang, F., Lai, J., Kao, L. 2003. Optimization of operation rule curves and flushing

654 schedule in a reservoir. Hydrol. Process. 17(8), 1623-1640

655 Chang, L., Chang, F., Wang, K., Dai, S. 2010. Constrained genetic algorithms for
656 optimizing multi-use reservoir operation. J. Hydrol. 390(1-2), 66-74.

657 Chen, L., Singh, VP, Lu, W., Zhang, J., Zhou, J., Guo, S. 2016. Streamflow forecast
658 uncertainty evolution and its effect on real-time reservoir operation. J. Hydrol.
659 540, 712-726.
660 Chen, J., Zhong, P., Zhang, Y., Navar, D., Yeh, W 2017. A decomposition -integration
661 risk analysis method for real-time operation of a complex flood control system.
662 Water Resour. Res., 53.
663 CWRC (Changjiang Water Resources Commission, Ministry of Water Resource).
664 2018. Joint operation rules for reservoirs in the upper and middle reaches of
665 Yangtze River (in Chinese).

666 Demarta S., McNeil A.J. 2005. The t copula and related copulas. Int. Stat. Rev. 73(1),
667 111-129.

668 Dembo R S, Eisenstat S C, Steihaug T. 1982. Inexact Newton Methods. Siam Journal
669 on Numerical Analysis, 19(2):400-408.
670 Ehteram, M., Mousavi, S.F., Karami, H., Farzin, S., Singh, V.P., Chau, K.W.,
671 El-Shafie, A., 2018. Reservoir operation based on evolutionary algorithms and
672 multi-criteria decision-making under climate change and uncertainty. J. Hydroinf.
673 20 (2), 332–355.
674 Franchini, M., Bernini, A., Barbetta, S., Moramarco, T. 2011. Forecasting discharges
675 at the downstream end of a river reach through two simple Muskingum based
676 procedures. J. Hydrol. 399(3), 335-352.
677 Gao, S., Liu, P., Pan, Z., Ming, B., Guo, S., Cheng, L., Wang, J. 2019. Incorporating
678 reservoir impacts into flood frequency distribution functions, J. Hydrol. 568,
679 234-246
680 Genest, C., Rémillard, B., 2008. Validity of the parametric bootstrap for
681 goodness-of-fit testing in semi-parametric models. Soc. Sci. Electron. Publish. 44
682 (6), 1096-1127.
683 Genest, C., Rémillard, B., Beaudoin, D., 2009. Goodness-of-fit tests for copulas: a
684 review and a power study. Insur. Math. Econ. 44 (2), 199-213.
685 Ghareb, A., Bakar, A., Hamdan, A. 2016. Hybrid feature selection based on enhanced
686 genetic algorithm for text categorization. Expert Systems with Applications,
687 49(1), 31-47.
688 Guo, S., Zhang, H., Chen, H., Peng, D., Liu, P., Pang, B., 2004. Reservoir flood
689 forecasting and control system in China. Hydrol. Sci. J. 49 (6), 959-972
690 Guo, S., Muhammad R., Liu, Z., Xiong, F., Yin, J. 2018. Design flood estimation
691 methods for cascade reservoirs based on copulas. Water. 10(5), 560.
692 Hao, C., Zhang, J., Yao, F. 2017. Multivariate drought frequency estimation using
693 copula method in southwest china. Theoretical and Applied Climatology,

694 127(977-991).
695 He, Y., Liu, R., Li, H., Wang, S., Lu, X. 2017. Short-term power load probability
696 density forecasting method using kernel-based support vector quantile regression
697 and copula theory. Appl. Energy. 185, 254-266.
698 Hofert, M., Pham, D. 2013. Densities of nested archimedean copulas. J. Multivariate
699 Anal. 118, 37-52.
700 Holland, J.H., 1975. Adaptation in Natural and Artificial Systems. The University of
701 Michigan Press, Ann Arbor, MI.
702 Hu, S. 1987. Determination of confidence intervals for design floods. J. Hydrol.
703 96(1-4), 201-213.

704 Hua, S. 1987. A general survey of flood-frequency analysis in China. J. Hydrol.
705 96(1-4), 15-25.

706 Huang, K., Ye L., Chen, L., Wang, Q., Dai, L., Zhou, J., Singh, VP., Huang, M.,
707 Zhang, J. 2018a. Risk analysis of flood control reservoir operation considering
708 multiple uncertainties. J. Hydrol. 565, 672-684.

709 Huang K. Chen, L., Zhou, J., Zhang, J., Singh, VP. 2018b. Flood hydrograph
710 coincidence analysis for mainstream and its tributaries. J. Hydrol. 565, 341-353.

711 Kim, D.H., Georgakakos, A.P. 2014. Hydrologic routing using nonlinear cascaded
712 reservoirs. Water Resour. Res. 50(8), 7000-7019.

713 Liang, Z., Huang, H., Cheng, L., Hu, Y., Yang, J., Tang, T. 2017. Safety assessment
714 for dams of the cascade reservoirs system of Lancang River in extreme situations.
715 Stoch. Environ. Res. Risk Assess. 1-11.

716 Liang, Z., Yang, J., Hu, Y., Wang, J., Li, B., Zhao, J. 2018. A sample reconstruction
717 method based on a modified reservoir index for flood frequency analysis of
718 non-stationary hydrological series. Stoch. Environ. Res. Risk Assess.
719 32:1561–1571

720 Li, X., Guo, S., Liu, P., Chen, G., 2010. Dynamic control of flood limited water level
721 for reservoir operation by considering inflow uncertainty. J. Hydrol. 391,
722 124-132.

723 Liu, P., Li, L., Guo, S., Xiong, L., Zhang, W., Zhang, J. 2015. Optimal design of
724 seasonal flood limited water levels and its application for the three gorges
725 reservoir. J. Hydrol. 527, 1045-1053.

726 Liu, X., Tang, Q., Voisin, N., Cui, H., 2016. Projected impacts of climate change on
727 hydropower potential in China. Hydrol. Earth Syst. Sci., 20, 3343-3359

728 López, J., Francés, F., 2013. Non-stationary flood frequency analysis in continental
729 Spanish rivers, using climate and reservoir indices as external covariates. Hydrol.
730 Earth Syst. Sci. 17, 3189-3203. https://doi.org/10.5194/hess-17-3189-2013

731 Lu, B., Gu, H., Xie, Z., Liu, J., Ma, L., Lu, W. 2012. Stochastic simulation for
732 determining the design flood of cascade reservoir systems. Hydrol. Res., 43,
733 54-63.

734 Mashal, R., Naldi, M., Zeevi, A. 2003. On the dependence of equity and asset returns.
735 Risk, 16, 83–87
736 MWR (Ministry of Water Resources), 2006. Regulation for calculating design flood
737 of water resources and hydropower projects. Water Resources and Hydropower
738 Press, Beijing, China (in Chinese).
739 Nelsen, R. 2006. An introduction to copulas, 2nd Edition. Springer-Verlag New York.
740 Ouyang, S., Zhou, J., Li, C., Liao, X., Wang, H., 2015. Optimal design for flood limit
741 water level of cascade reservoirs. Water Resour. Manage. 29 (2), 445–457.
742 Pilanci, M., Wainwright, M. J. 2017. Newton sketch: a linear-time optimization
743 algorithm with linear-quadratic convergence. Siam J. Optim. 27(1), 205-245.
744 Rivieccio, G., De Luca, G. 2016. Copula function approaches for the analysis of serial
745 and cross dependence in stock returns. Finance Research Letters, 17, 55-61
746 Salvadori G., De Michele, C. 2004. Frequency analysis via copulas: Theoretical
747 aspects and applications to hydrological events. Water Resour. Res. 40, 229-244

748 Salvadori, G.; Durante F.; De Michele, C.; Bernardi M.; Petrella L. 2016. A
749 multivariate Copula-based framework for dealing with Hazard Scenarios and
750 Failure Probabilities. Water Resour. Res. 52, 3701-3721,

751 Salvadori, G.; De Michele, C.; Durante, F. 2011. On the return period and design in a
752 multivariate framework. Hydrol. Earth Syst. Sci. 15, 3293-3305.

753 Serinaldi F, Grimaldi S. 2007. Fully nested 3-copula: procedure and application on
754 hydrological data. J. Hydrol. Eng. 12(4), 420-430

755 Serinaldi, F., Bonaccorso, B., Cancelliere, A., Grimaldi, S. 2009. Probabilistic
756 characterization of drought properties through copulas. Phys. Chem. Earth.
757 34(10-12), 596-605.

758 Su, C., Chen, X. 2019 Assessing the effects of reservoirs on extreme flows using
759 nonstationary flood frequency models with the modified reservoir index as a
760 covariate. Adv. in Water Resour. 124, 29-40

761 Vyver, H. V. D., Bergh, J. V. D. 2018. The Gaussian copula model for the joint deficit
762 index for droughts. J. Hydrol.561, 978-999

763 Wang, W., Li, H.Y., Leung, L.R., Yigzaw, W., Zhao, J., Lu, H. et al. 2017. Nonlinear
764 filtering effects of reservoirs on flood frequency curves at the regional scale.
765 Water Resour. Res. 53, 8277-8292

766 Xiao, Y., Guo, S., Liu, P., Yan, B., Chen, L. 2009. Design flood hydrograph based on
767 multi-characteristic synthesis index method. J. Hydrol. Eng. 14(12), 1359-1364.

768 Xie, A., Liu, P., Guo, S., Zhang, X., Jiang, H., Yang, G. 2018. Optimal design of
769 seasonal flood limited water levels by jointing operation of the reservoir and
770 floodplains. Water Resour. Manag. 32(1), 1-15.

771 Xiong F, Guo S, Chen L, Yin J, Liu P 2018. Flood frequency analysis using Halphen
772 distribution and maximum entropy. J. Hydrol. Eng. 23(5): 04018012

773 Xiong F, Guo S, Chen L, Chang F.J., Zhong Y., Liu P. 2019. Identification of flood
774 seasonality using an entropy-based method, Stoch. Environ. Res. Risk Assess.
775 32:3021-3035

776 Yan J. 2007. Enjoy the joy of copulas: with a package copula. J. Stat. Softw. 21:1-21.

777 Yazdi J., Moridi A. 2018. Multi-objective differential evolution for design of cascade
778 hydropower reservoir systems. Water Resour. Manag. 32:4779-4791.

779 Yin, J., Guo, S., Liu, Z., Yang, G., Zhong, Y., Liu, D. 2018. Uncertainty analysis of
780 bivariate design flood estimation and its impacts on reservoir routing. Water
781 Resour. Manag. 32(5), 1795-1809.

782 Yin, Z., Wen, X., Feng, Q., He, Z., Zou, S., Yang, L., 2017. Integrating genetic
783 algorithm and support vector machine for modeling daily reference
784 evapotranspiration in a semi-arid mountain area. Hydrol. Res. 48 (5), 1177-1191

785 Yun, R., Singh, V.P., 2008. Multiple duration limited water level and dynamic limited
786 water level for flood control, with implication on water supply. J. Hydrol. 354
787 (1-4), 160-170.

788 Zhang, L., Singh, V.P. 2007. Bivariate rainfall frequency distributions using
789 Archimedean copulas. J. Hydrol. 332(1), 93-109.

790 Zhang, J., Lin, X., Guo, B. 2016. Multivariate copula-based joint probability
791 distribution of water supply and demand in irrigation district. Water Resour.
792 Manag. 30(7), 2361-2375.

793 Zhang, Q., Gu, X., Singh, V.P., Xiao, M., Chen, X., 2015. Evaluation of flood
794 frequency under non-stationarity resulting from climate indices and reservoir
795 indices in the east river basin, China. J. Hydrol. 527, 565-575.

796 Zhao, G., Gao, H., Naz, B. S., Kao, S. C., Voisin, N. 2016. Integrating a reservoir
797 regulation scheme into a spatially distributed hydrological model. Adv. Water
798 Resour. 98, 16-31.

799 Zhong, Y., Guo, S., Liu, Z., Wang, Y., Yin, J. 2017. Quantifying differences between
800 reservoir inflows and dam site floods using frequency and risk analysis methods.
801 Stoch. Environ. Res. Risk Assess. (6), 1-15.

802 Zhong, Y., Guo, S., Ba, H., Xiong, F., Chang, F.J., Lin, K. 2018. Evaluation of the
803 BMA probabilistic inflow forecasts using TIGGE numeric precipitation

predictions based on artificial neural network. Hydrol. Res. 49 (5), 1417-1433.

Zhou, Y., Guo, S., Xu, C. Y., Liu, P., Qin, H. 2015. Deriving joint optimal refill rules for cascade reservoirs with multi-objective evaluation. J. Hydrol., 524(3), 166-181.

Zhou, Y., Chang, L., Uen, T., Guo, S., Xu, C-Y., Chang, F. 2019 Prospect for small-hydropower installation settled upon optimal water allocation: An action to stimulate synergies of water-food-energy nexus. Appl. Energy. 238, 668-682

https://doi.org/10.1016/j.jhydrol.2019.124003

List of Tables

842 Table 1 Similarities and differences between design flood in construction and
843 operation periods.

	Construction period	Operation period
Purpose	Provide vital information for the design of the reservoir storage, spillway size etc.	Provide vital information for reservoir multi-objective operation
Property	A static value unchanged over time	A static value unchanged over time
Analysis method	Statistical analysis (Flood frequency analysis)	Statistical analysis combined with consideration of reservoir operation rules
Application results	(1) Determine FLWL in construction period (2) Reservoir can withstand the design frequency floods in construction period. (3) There exist enormous conflicts between flood control and conservation.	(1) Determine FLWL in operation period. (2) Reservoir can withstand the same design frequency floods regulated by upstream reservoirs. (3) Tradeoff between flood control and conservation.

844

845 Table 2 Comparison of EFRC and MLRC in terms of synthetic AM flood series with
846 different correlation coefficients (R).

R	1000-year design inflow of A2	Methods	A1 inflow	B1 inflow
0.01	213.1	MLRC	52.5	160.6
		EFRC	125.1	88
0.3	213.7	MLRC	99.2	114.5
		EFRC	126.7	87
0.6	212.5	MLRC	113.6	98.9
		EFRC	124.8	87.7
0.99	214.1	MLRC	127.8	86.3
		EFRC	127.9	86.2

847

848 Table 3 Basic information of cascade reservoirs in the Jinsha River and Yalong River

Region	Midstream Jinsha River						Yalong River			Downstream Jinsha River			
Reservoir	LY	AH	JAQ	LKK	LDL	GYY	LHK	JP	ET	WDD	BHT	XLD	XJB
Drainage area (thousand km^2)	220	235.4	237.4	240	247.3	256.5	65.6	102.6	116.4	406.1	430.3	454.4	458.8
Normal pool level（m）	1618	1504	1418	1298	1223	1134	2865	1880	1200	975	825	600	380
Flood limited water level (m)	1605	1493	1410	1289	1212	1122.3	2845	1859	1190	952	785	560	370
Design flood water level (m)	1618	1504	1418	1298	1223	1134	2865	1880.5	1200	979.38	827.71	604.23	380
Flood control storage（billion m^3）	0.17	0.22	0.16	0.13	0.56	0.54	2.00	1.61	0.94	2.44	7.50	4.65	0.90
Total storage capacity (billion m^3)	0.81	0.89	0.91	0.56	1.72	2.25	10.77	7.99	5.80	3.94	20.60	12.67	5.16
Installed hydropower capacity (GW)	2.40	2.00	2.40	1.80	2.16	3.00	3.00	3.60	3.30	10.20	16.00	13.86	7.75
Daily data record length	1939-2007	1939-2007	1939-2007	1939-2007	1950-2007	1950-2007	1950-2007	1950-2007	1950-2007	1950-2007	1942-2007	1950-2007	1950-2007

849

Table 4 Goodness-of-fit statistics of t-copula for MLRC of GYY reservoir.

Degrees of freedom	KS (*P*-value)	CM(*P*-value)	RMSE	AIC
v=2	0.93	0.47	0.018	-392.24
v=3	0.94	0.49	0.017	-393.73
v=4	0.94	0.48	0.017	-393.69
v=5	0.92	0.48	0.017	-393.60

Table 5. Flood regional composition results at GYY reservoir site.

Return period (year)	Inflow of GYY (10^8m^3)	Methods	LY reservoir inflow (10^8m^3)	L-A inter-basin inflow (10^8m^3)	A-J inter-basin inflow (10^8m^3)	J-L inter-basin inflow (10^8m^3)	L-L inter-basin inflow (10^8m^3)	L-G inter-basin inflow (10^8m^3)
1000	86.49	MLRC	66.97	7.95	1.02	1.36	3.78	5.41
		EFRC	67.64	7.62	1.01	1.32	3.85	5.05
500	81.55	MLRC	63.14	7.50	0.96	1.28	3.56	5.10
		EFRC	63.77	7.19	0.95	1.25	3.63	4.76
100	69.74	MLRC	54.00	6.41	0.82	1.10	3.05	4.36
		EFRC	54.54	6.14	0.82	1.06	3.10	4.08

858 Table 6 Comparison of Guo's method and proposed method for deriving MLRC of AH and LDL reservoirs.

Investigated reservoir	1000-year design inflow(10^8m^3)	MLRC	Guo's method	Proposed method
AH reservoir	75.26	LY reservoir inflow(10^8m^3)	67.32	67.38
		L-A inter-basin inflow(10^8m^3)	7.94	7.88
LDL reservoir	81.44	LY reservoir inflow(10^8m^3)	no solution	67.26
		L-A inter-basin inflow(10^8m^3)		7.84
		A-J inter-basin inflow(10^8m^3)		1.05
		J-L inter-basin inflow(10^8m^3)		1.32
		L-L inter-basin inflow(10^8m^3)		3.97

859
860

Table 7 Comparison of design frequency floods in construction and operation periods for the cascade reservoirs in the midstream Jinsha River and Yalong River.

Variable	Period	LY	AH	JAQ	LKK	LDL	GYY	LHK	JP	ET
Return period (year)		500	500	500	500	500	500	1000	1000	1000
Q_{max} (m^3/s)	construction	12200	14400	14700	15730	15900	16900	9700	13570	20620
	operation	12200	13590(-5.6%)	13625(-7.3%)	14550(-7.5%)	14634(-8%)	14957(-11.5%)	9700	11370(-16.2%)	16240(-21.2%)
W_3 (10^8m^3)	construction	30.1	35.4	36.1	38.8	39.1	41.2	24.9	34.8	52.9
	operation	30.1	34.1(-3.8%)	34.2(-5.4%)	36.7(-5.5%)	36.7(-6.1%)	37.2(-9.7%)	24.9	29.7(-14.7%)	42.4(-19.8%)
W_7 (10^8m^3)	construction	63.8	70.9	71.9	73.2	76.8	81.6	55.3	77.3	117.5
	operation	63.8	69.8(-1.6%)	69.9(-2.8%)	70.9(-3.2%)	74(-3.7%)	75.6(-7.3%)	55.3	70.6(-8.7%)	97.9(-16.7%)
W_{30} (10^8m^3)	construction	228	268	273	292	300	306	161	225.8	343.2
	operation	228	268(-0%)	273(-0%)	292(-0%)	300(-0%)	304.7(-0.4%)	161	225.8(-0%)	340.6(-0.8%)
FLWL(m)	construction	1605	1493.3	1410	1289	1212	1122.3	2845	1859	1190
	operation	1605	1493.7	1410.8	1290.3	1212.8	1123.5	2845	1862.4	1191.6
HG(10^8kW.h)	construction	14.88	13.22	15.25	11.32	13.16	18.01	19.32	23.39	21.36
	operation	14.88	13.28(+0.45%)	15.36(+0.72%)	11.55(+2%)	13.3(+1.1%)	18.23(+1.2%)	19.32	23.76(+1.6%)	21.49(+0.6%)

865

866 Table 8. Flood regional composition results at XJB reservoir site.

867

Return period (year)	Inflow of XJB (10^8m^3)	Methods	GYY reservoir inflow (10^8m^3)	ET reservoir inflow (10^8m^3)	G-E-W inter-basin inflow (10^8m^3)	W-B inter-basin inflow (10^8m^3)	B-X inter-basin inflow (10^8m^3)	X-X inter-basin inflow (10^8m^3)
1000	237	MLRC	85.89	75.78	18.95	20.90	33.06	2.42
		EFRC	86.49	74.93	18.73	21.89	32.86	2.20
500	223	MLRC	81.08	71.44	17.86	19.64	30.64	2.34
		EFRC	81.55	70.41	17.60	20.61	30.54	2.07
100	189	MLRC	69.19	60.40	15.10	16.25	25.98	2.07
		EFRC	69.74	59.64	14.91	17.54	25.07	1.75

868

https://doi.org/10.1016/j.jhydrol.2019.124003

Table 9 Comparison of 1000-year design floods in construction and operation periods for the cascade reservoirs in the downstream Jinsha River

Variable	Period	WDD	BHT	XLD	XJB
Q_{max}(m^3/s)	construction	35800	38800	43300	43700
	operation	25450(-28.9%)	27134(-30%)	29149(-32.7%)	26807(-38.7%)
W_3(10^8m^3)	construction	87.4	95.2	106	108
	operation	66.7(-23.7%)	69.8(-26.7%)	72.1(-32%)	67.6(-37.4%)
W_7(10^8m^3)	construction	181	202	235	237
	operation	148.2(-18.1%)	160.8(-20.4%)	165.9(-29.4%)	155.9(-34.2%)
W_{30}(10^8m^3)	construction	542	682	752	759
	operation	521.9(-3.7%)	652.7(-4.3%)	694.1(-7.7%)	654.3(-13.8%)
FLWL(m)	construction	952	785	560	370
	operation	958.01	793.6	572.71	372.09
HG(10^8kW.h)	construction	133.1	197.7	190.5	97
	operation	139.3(+4.7%)	207.1(+4.8%)	204.3(+7.2%)	99.1(+2.2%)

Table 10 Kendall's tau correlation coefficients between AM 7d flood volumes of cascade reservoirs in the midstream Jinsha River

Reservoir	LY	AH	JAQ	LKK	LDL	GYY
LY	1	0.91	0.89	0.88	0.83	0.78
AH	0.91	1	0.98	0.97	0.92	0.86
JAQ	0.89	0.98	1	0.98	0.93	0.88
LKK	0.88	0.97	0.98	1	0.94	0.89
LDL	0.83	0.92	0.93	0.94	1	0.92
GYY	0.78	0.86	0.88	0.89	0.92	1

List of Figures

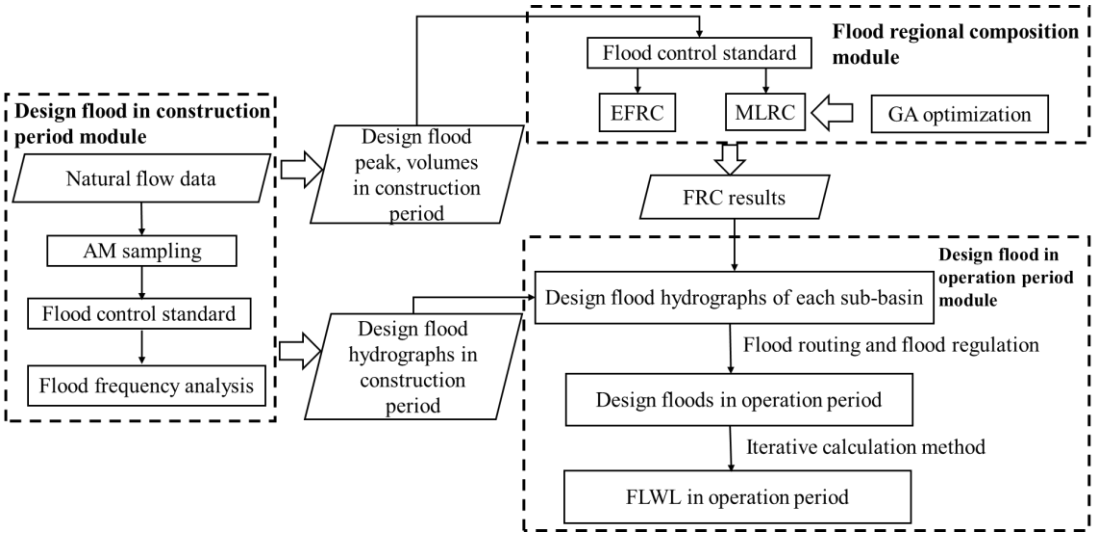

Fig. 1 Framework depicting the design flood for cascade reservoirs in operation period

914

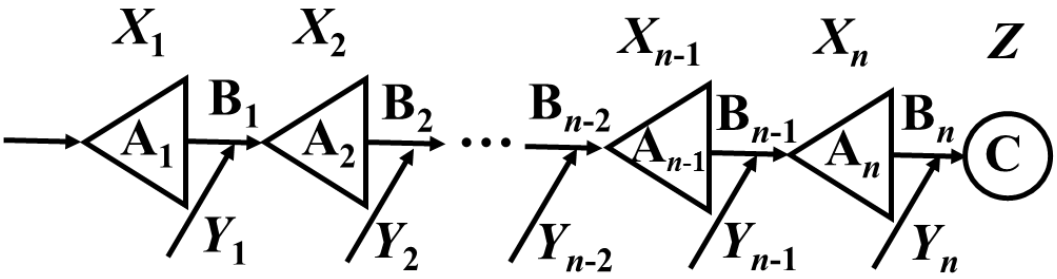

915

916 Fig. 2 Sketch diagram of cascade reservoir system

917

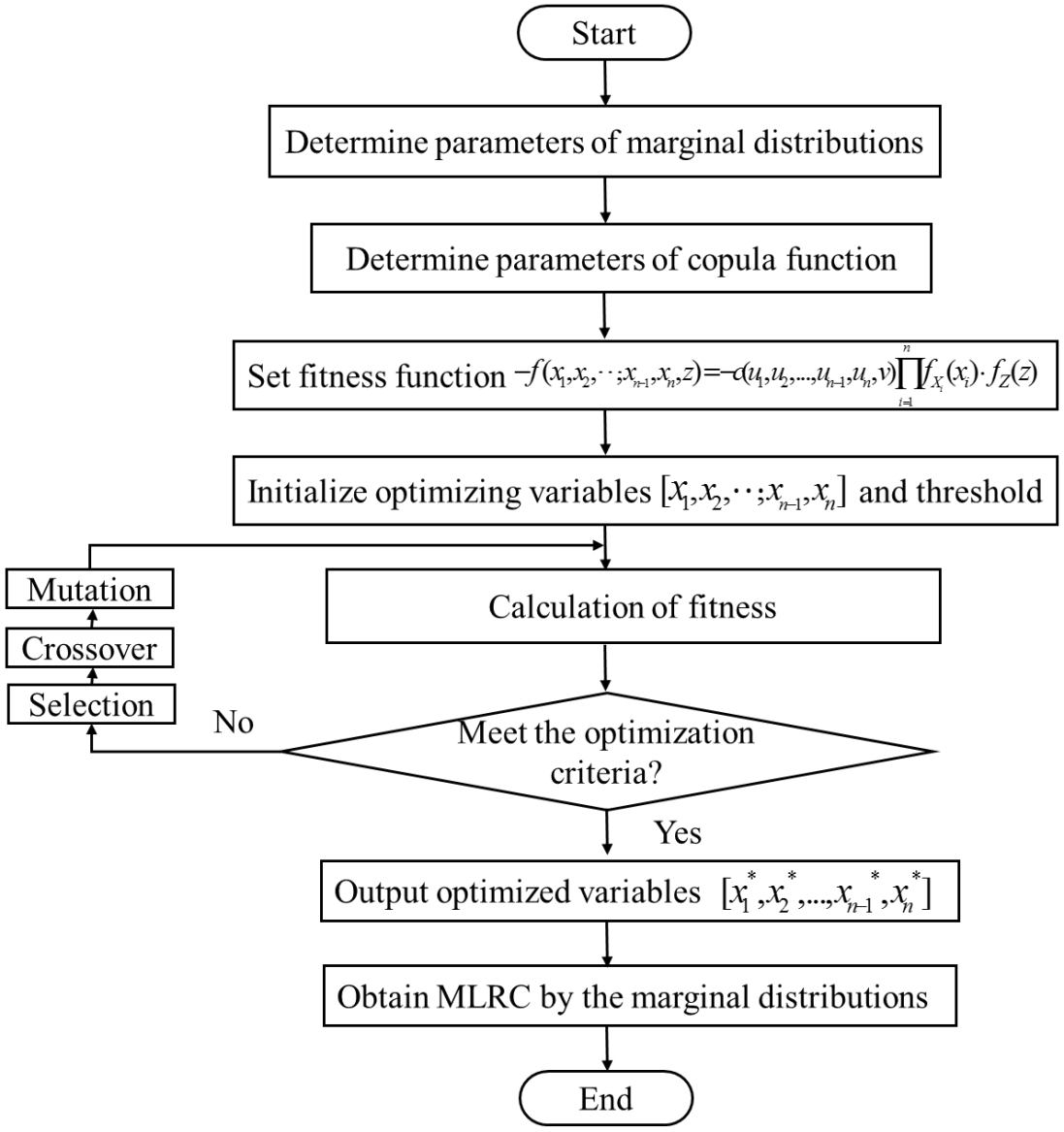

Fig. 3 Flow chart for genetic algorithm (GA) based derivation of MLRC

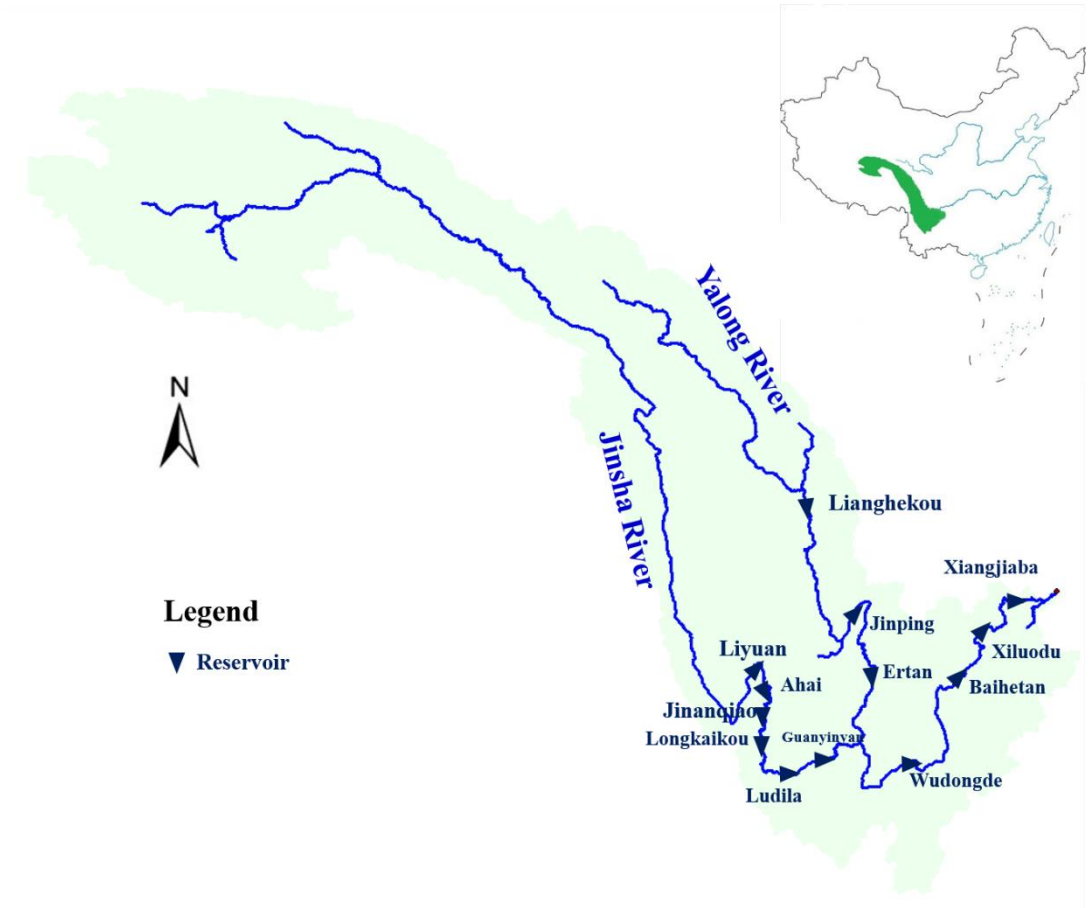

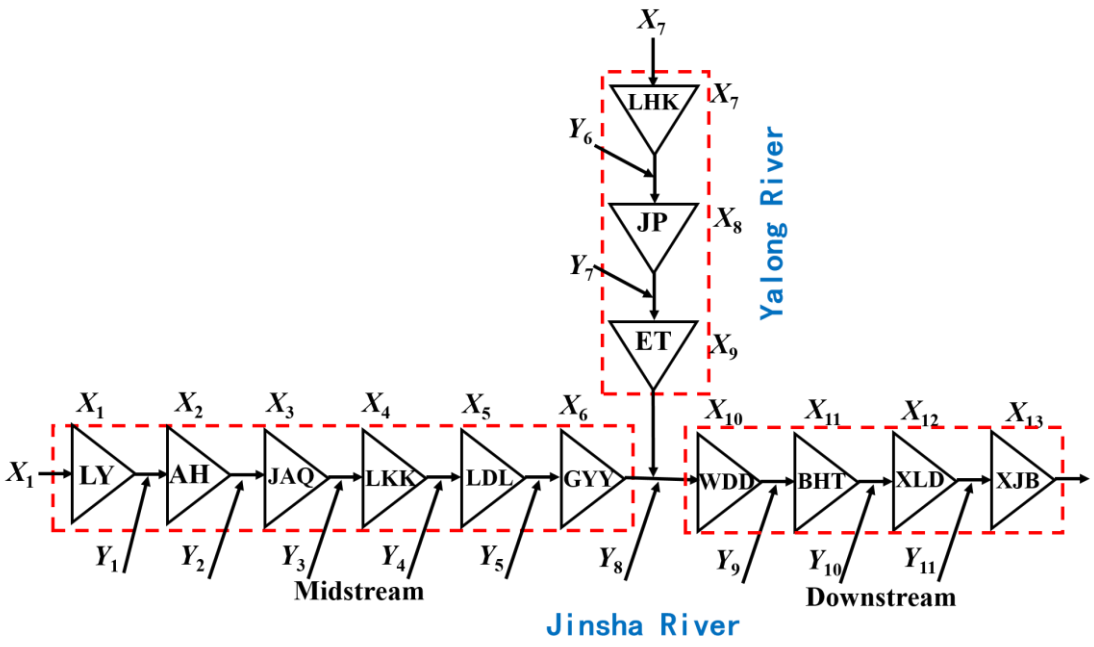

Fig.4 Sketch map of investigated area and cascade reservoirs in the Jinsha River and Yalong River

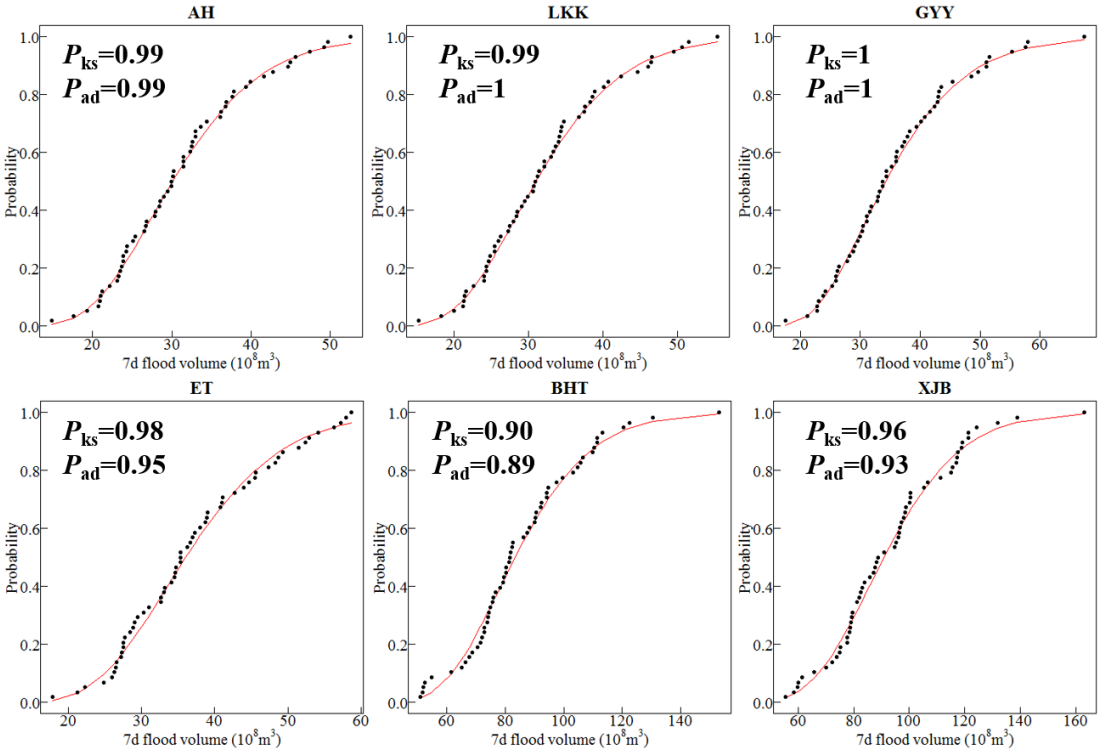

Fig. 5 Cumulative distributions of 7d AM flood volumes series fitted by P3 distributions for AH, LKK, GYY, ET, BHT and XJB reservoirs, on which P_{ks} and P_{ad} denote the corresponding *P*-value of KS test and AD test, respectively.

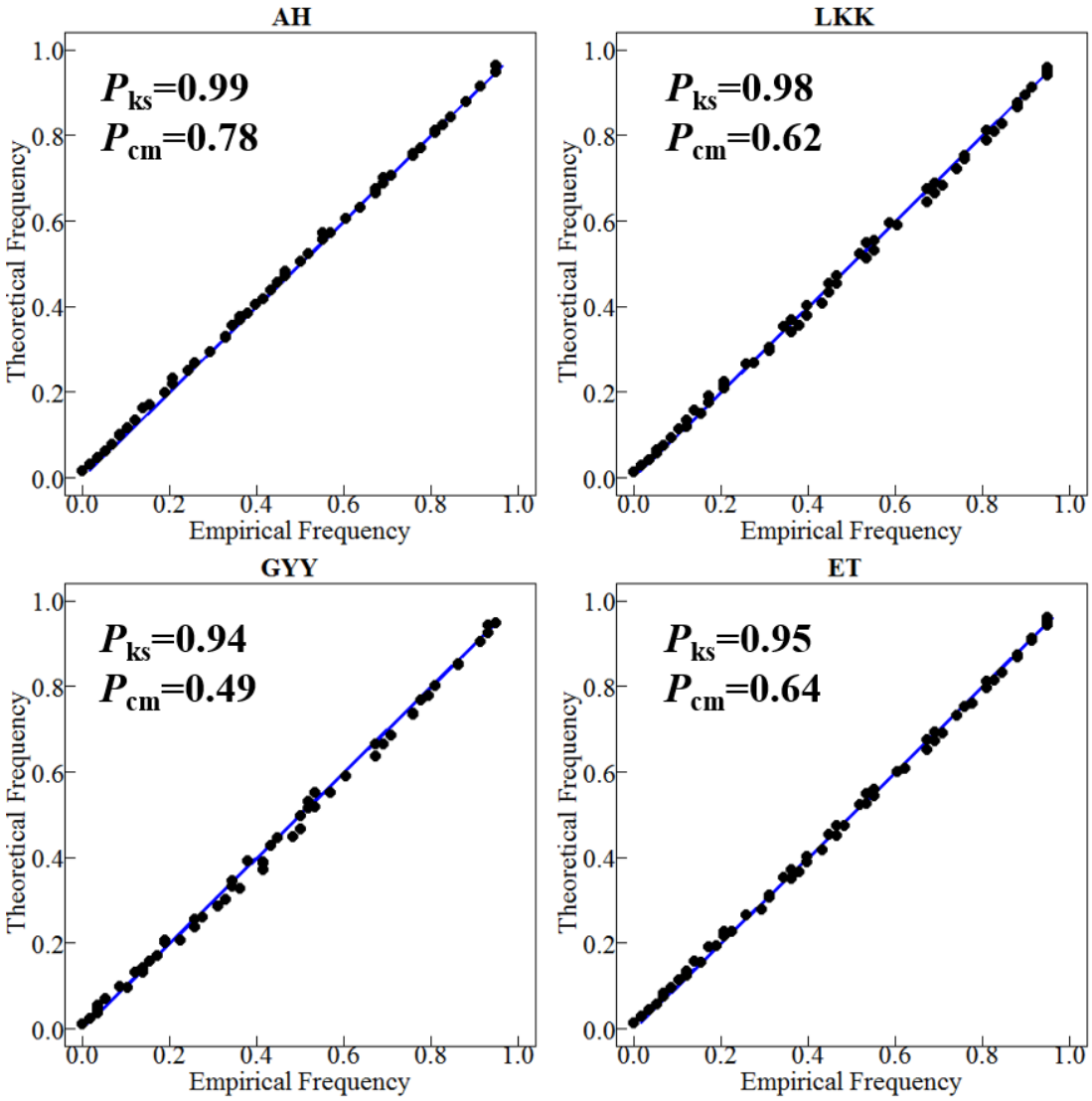

Fig. 6 The P-P plots fitted by the joint distributions for the MLRC of 7d flood volumes of AH, LKK, GYY and ET reservoirs, on which P_{ks} and P_{cm} denote the corresponding *P*-value of KS test and CM test, respectively.

940

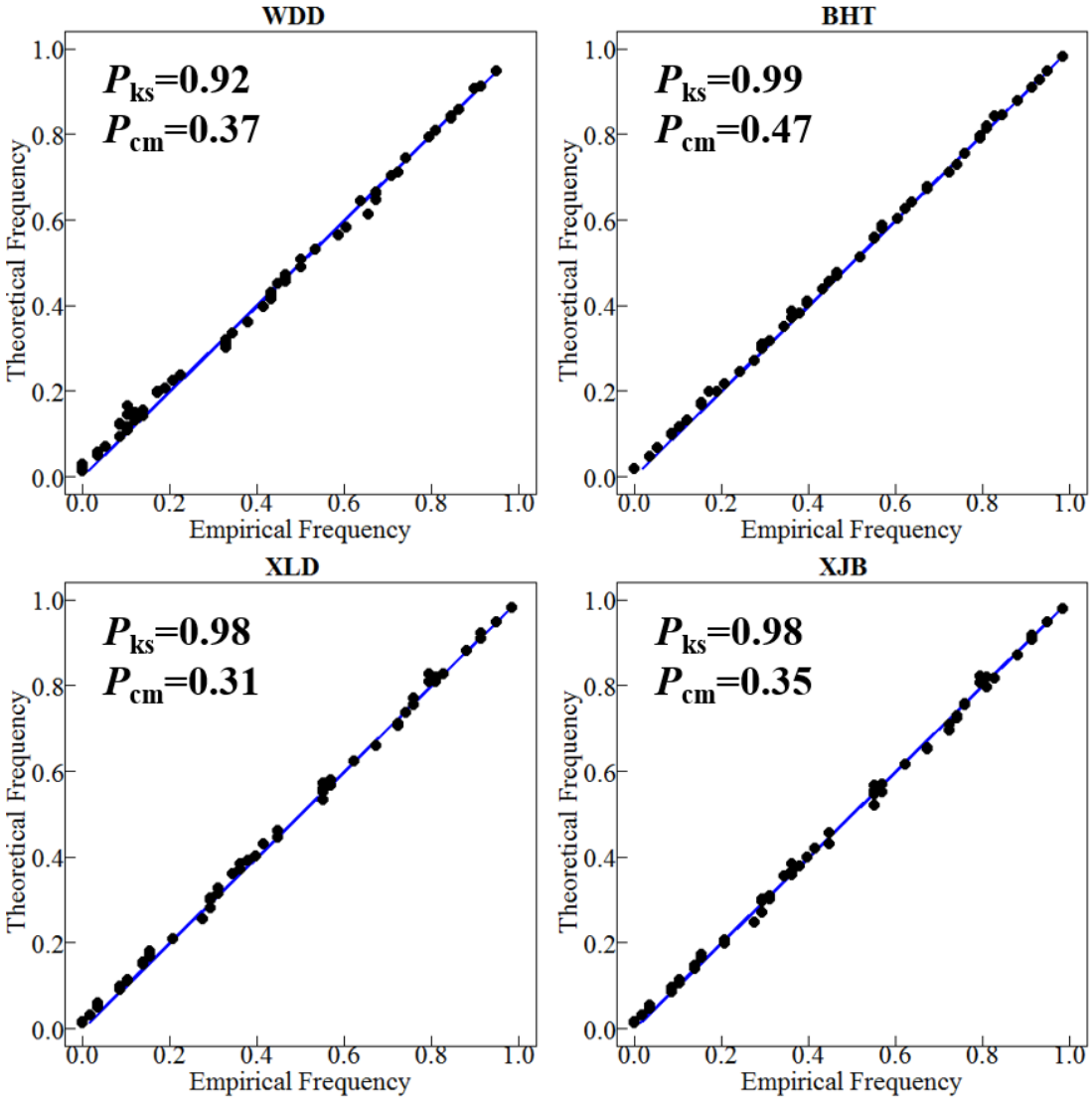

941

942 Fig. 7 The P-P plots fitted by the joint distributions for the MLRC of 7d flood
943 volumes of WDD, BHT, XLD and XJB reservoirs, on which P_{ks} and P_{cm} denote the
944 corresponding *P*-value of KS test and CM test, respectively.

945

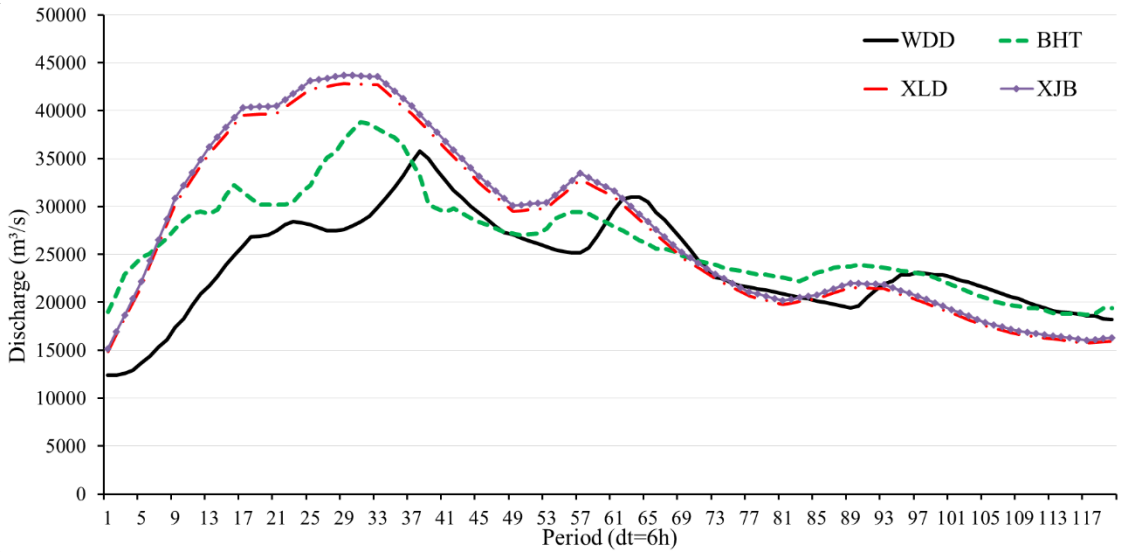

(a) Design flood hydrographs in construction period

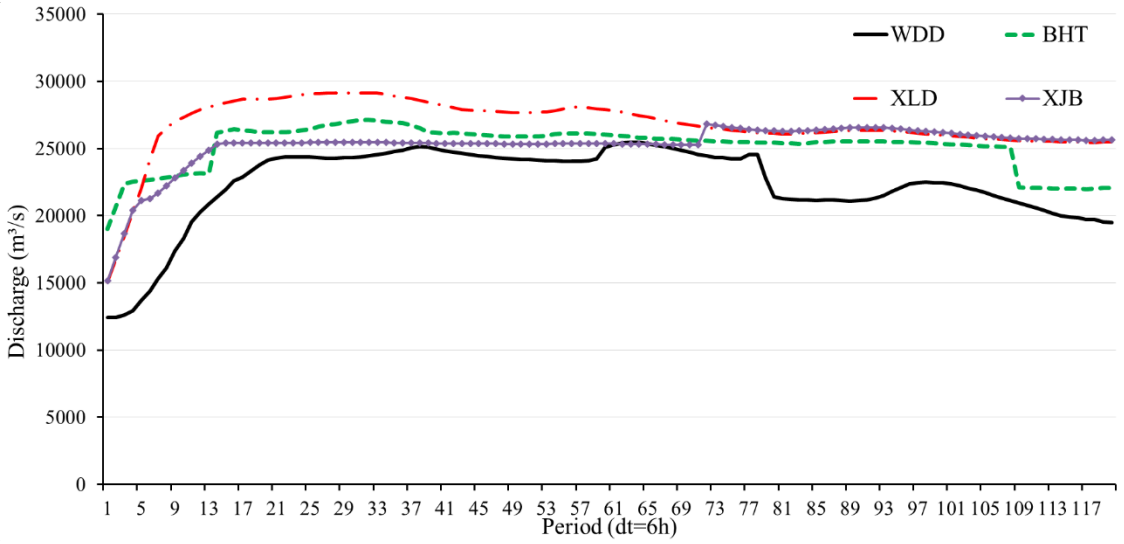

(b) Design flood hydrographs in operation period

Fig. 8 1000-year design flood hydrographs of cascade reservoirs in the downstream Jinsha River.

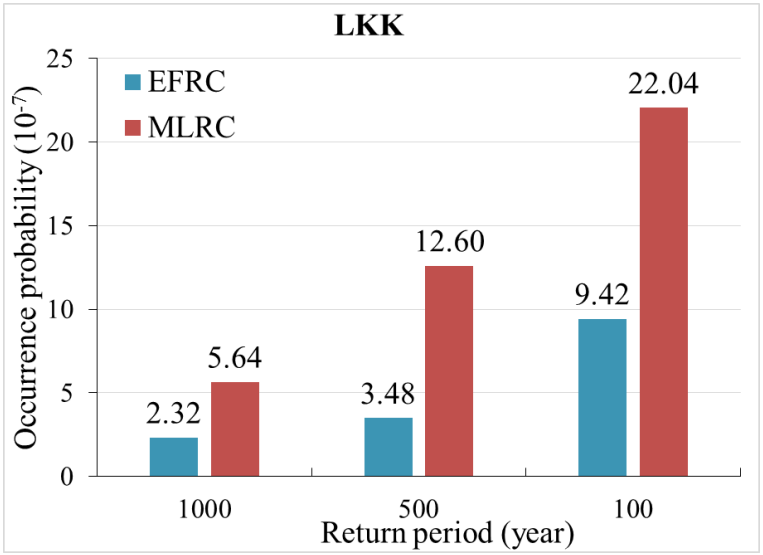

(a) LKK reservoir

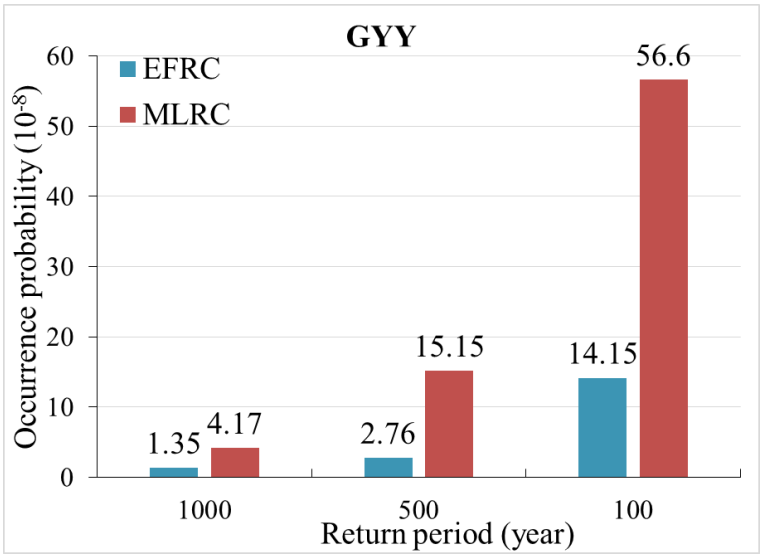

(b) GYY reservoir

Fig. 9 Comparison of the occurrence probability of EFRC and MLRC of LKK and GYY reservoirs.

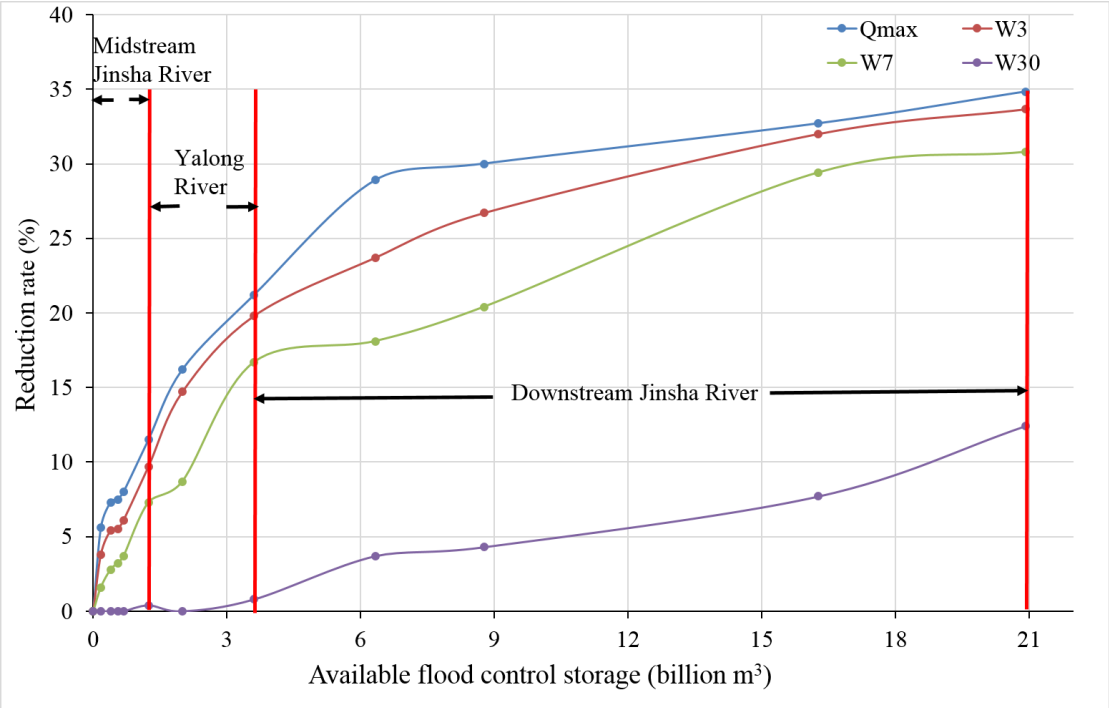

960

961 Fig. 10 Relation between reduction rate and available flood control storage

962